On three- and two-dimensional fiber distributed models of biological tissues

Marcello Vasta [a,*], Alessio Gizzi [b], Anna Pandolfi [c]

[a] Università di Pescara-Chieti, Dipartimento PRICOS, Viale Pindaro 42, Pescara, Italy
[b] University Campus Bio-Medico of Rome, Engineering Faculty, Via A. del Portillo 21, Rome, Italy
[c] Politecnico di Milano, Dipartimento di Ingegneria Civile ed Ambientale, Piazza Leonardo da Vinci 32, Milano, Italy

Article history:
Received 15 March 2013
Received in revised form
13 December 2013
Accepted 23 May 2014
Available online 11 June 2014

1. Introduction

The theoretical and numerical modeling of the mechanical behavior of soft biological tissues in physiological or pathological conditions has received particular attention in the last few decades. One of the reasons of the interest is the necessity to use numerical models in medicine and biology to predict the behavior of organs or biological ensembles. Another reason is the design and the improvement of diagnostic tools and instruments that interact with biological tissues. Another motivation is the invention and the development of new materials mimicking peculiar features observed in natural tissues. The definition of a numerical model involving bio-tissues requires, in addition to the accurate measurements of the geometry, the use of sophisticated material models that must be calibrated against ad hoc experimental data. Note that the parameters of a material model are individual-dependent and often cannot be transferred easily from one case to another. Therefore, in view of actual applications, it seems to be wise to pursue the definition of material models with a reduced number of material parameters but otherwise able to cover a large range of deformations. In this way the calibration of the parameters may be somehow facilitated. The search of accurate material models characterized by a few material parameters is one of the key aspects of the modern computational biomechanics, and the present study tries to give a contribution by including the natural randomness of soft biological tissues.

In many situations of practical interest the non-pathological behavior of biological tissues is described sufficiently well by hyperelastic models that have been conceived for rubber materials, e.g., neo-Hookean, Mooney–Rivlin, Yeoh and others. On the other hand, most biological tissues are characterized by anisotropy, necessarily because the organ must provide a general multi-direction confinement and, at the same time, it must resist to localized and strongly oriented actions. Mechanical anisotropy is achieved by means of complex and specialized architectures of cable-like fibrils and fibers, made of the most diffused protein in nature, i.e., the collagen. It follows that material models commonly employed for biological tissues account for different kinds of anisotropy induced by the collagen cables [10,18,5,13,8]. Moreover, biological tissues are characterized ineluctably by a spatial distribution of the collagen reinforcement whereas unique strong alignments of fibers are in contrast with the function of the organ. Examples of distributed reinforcing fibers are found in the microstructure of the cornea [4,15,16,2] and of the artery walls, and in other biological tissues [7,17]. In the recent literature numerous material models considering a distributed orientation of the collagen fibers have been presented and discussed, starting from the seminal work by Lanir [14], and including several important contributions [7,6,1]. In this regard, our recent work on this field [19] proposed a novel point of view by introducing the concept of second order (or variance) approximation of the strain energy density of a fiber distributed material in terms of the fourth pseudo-invariant $\bar{I}_4$. The model was developed to overcome the

* Corresponding author.
E-mail addresses: mvasta@unich.it (M. Vasta), a.gizzi@unicampus.it (A. Gizzi), anna.pandolfi@polimi.it (A. Pandolfi).

two main difficulties of non-deterministic mechanical properties: (i) the impossibility to obtain the analytical definition of stress and elasticity tensors and (ii) the heavy computational effort necessary to compute stress and elasticity tensors in numerical applications.

Statistically based material models are appealing in stochastic approaches when they are proved to perform well also in terms of covariance stress tensors. The discussion on the covariance stress tensor of the second order approximation model is one of the new contributions of the present paper on the line of [23].

In several tissues geometrically organized as structures, e.g., skin, corneas, irides, artery walls, and other shell-like or membrane like organs, the distribution of the collagen fibers assumes a prevailing two-dimensional configuration [2,20]. The attractive possibility of using membrane and shell theories to reduce the computational effort in view of evaluating the mechanical behavior of organs calls for the development of constitutive models characterized by planarity of the fiber micro-structural organization, see, e.g., [21,24]. As an additional new contribution of this work, we present here the two-dimensional version of the second order approximation material model above recalled [19].

The organization of the paper is as follows. In Section 2 we introduce briefly the hyperelastic framework and the necessary definitions. In Section 3 we recall the basic ideas of the three-dimensional material model presented in [19]. Under the assumption of an axis-symmetric distribution of the fiber orientation, we derive a particularly compact analytical expression of the second Piola–Kirchhoff stress and of the covariance stress tensor. In Section 4 we particularize the three-dimensional model to a specific plane, containing the distribution of fibers. In Section 5 we compare, through uniaxial, biaxial and shear test, the behavior of the two-dimensional and three-dimensional distributions, in terms of stress and covariance stress components. The behavior of the model as a function of concentration parameter of a von Mises distribution is also discussed.

2. Hyperelasticity framework

In the framework of nonlinear continuum mechanics, we postulate the existence of a Helmholtz free-energy density per unit reference volume Ψ. We comply with the purely elastic case, where the free energy is assumed to be dependent on the deformation gradient $\mathbf{F}$ only, i.e., $\Psi = \Psi(\mathbf{F})$. For a biological tissue with collagen fibers it is customary to decompose additively the strain energy into three terms:

$$\Psi = \Psi_{\text{vol}} + \Psi_{\text{iso}} + \Psi_{\text{aniso}}. \tag{1}$$

The first term, Ψ_{vol}, accounts for volume changes, and it is assumed to be dependent on the volumetric part of the deformation, i.e., on the Jacobian $J = \det \mathbf{F}$, i.e.,

$$\Psi_{\text{vol}} = \Psi_{\text{vol}}(J).$$

The second term, Ψ_{iso}, accounts for the isotropic behavior of the material due to the underlying matrix and eventually to a portion of isotropically distributed fibrous reinforcement. Usually, Ψ_{iso} is assumed to be dependent on the first and second invariants, $\bar{I}_1$ and $\bar{I}_2$, of the modified Cauchy–Green deformation tensor $\overline{\mathbf{C}} = \overline{\mathbf{F}}^T \overline{\mathbf{F}}$, where $\overline{\mathbf{F}} = J^{-1/3}\mathbf{F}$:

$$\Psi_{\text{iso}} = \Psi_{\text{iso}}(\bar{I}_1, \bar{I}_2).$$

The anisotropic effect of the fibrous reinforcement is described by the third term Ψ_{aniso}. According to a standard approach initiated by Spencer [22], here Ψ_{aniso} is assumed to be dependent on the modified tensor $\overline{\mathbf{C}}$ and on particular vectors – or tensors – describing the intrinsic microstructure of the material. As a consequence of the additive decomposition (1) and of the decoupling of the arguments between the addends, it follows that the second Piola–Kirchhoff stress tensor $\mathbf{S}$ splits into the sum of three terms:

$$\mathbf{S} = \mathbf{S}_{\text{vol}} + \mathbf{S}_{\text{iso}} + \mathbf{S}_{\text{aniso}},$$

in the form:

$$\mathbf{S} = 2\frac{\partial \Psi}{\partial \mathbf{C}} = 2\frac{\partial \Psi_{\text{vol}}}{\partial \mathbf{C}} + (\overline{\mathbf{S}}_{\text{iso}} + \overline{\mathbf{S}}_{\text{aniso}})\frac{\partial \overline{\mathbf{C}}}{\partial \mathbf{C}},$$

where

$$\overline{\mathbf{S}}_{\text{iso}} = 2\frac{\partial \Psi_{\text{iso}}}{\partial \overline{\mathbf{C}}}, \quad \overline{\mathbf{S}}_{\text{aniso}} = 2\frac{\partial \Psi_{\text{aniso}}}{\partial \overline{\mathbf{C}}}. \tag{2}$$

Explicit expressions for the anisotropic second Piola–Kirchhoff stress can be found in standard continuum mechanics textbooks [9].

According to [10], in the case of a single family of parallel fibers oriented in the referential direction $\mathbf{a}_0$, a well accepted form of the anisotropic Helmholtz free energy density is given by

$$\Psi_{\text{aniso}}(\bar{I}_4) = \overline{\Psi}_{\text{aniso}}(\bar{I}_4) + \Psi^0_{\text{aniso}} = \frac{k_1}{2k_2}\exp[k_2(\bar{I}_4 - 1)^2] - \frac{k_1}{2k_2},$$

where the pseudo-invariant $\bar{I}_4$ is the contraction of $\overline{\mathbf{C}}$ and of the second order structure tensor $\mathbf{A}_0 = \mathbf{a}_0 \otimes \mathbf{a}_0$, i.e.,

$$\bar{I}_4(\mathbf{a}_0) = \overline{\mathbf{C}} : \mathbf{A}_0.$$

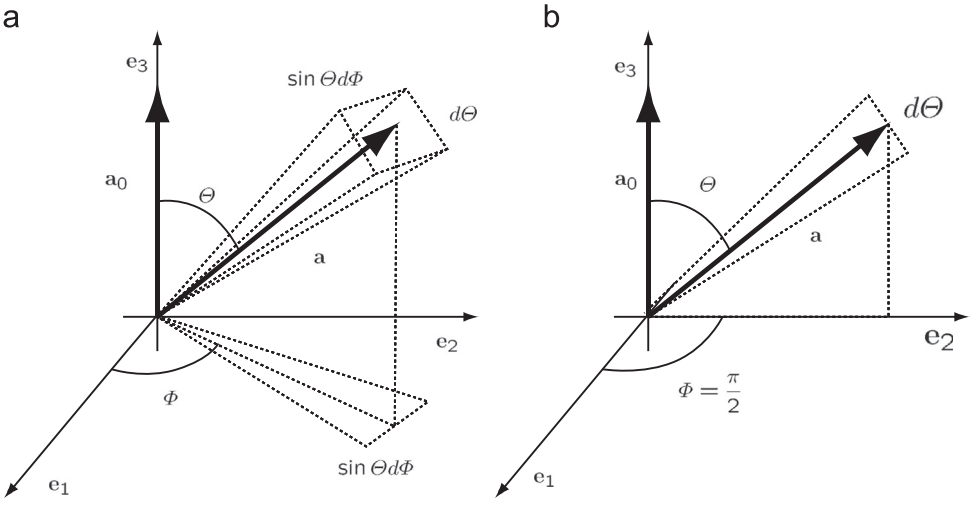

Fig. 1. Orientation of the generic unit vector **a** aligned with a portion of fibers. (a) Spherical coordinates for a fully three-dimensional distribution. (b) Cylindrical coordinates for a planar distribution.

The invariant $\bar{I}_4$ represents the square of the stretch along the original direction $\mathbf{a}_0$. Since the contribution of the fibers can be accounted for only when they are in extension, the anisotropic contribution to the energy must be considered if and only if $\bar{I}_4 > 1$, otherwise it must be set equal to zero. Alternative forms of the reinforcing energy, based on polynomial functions [12] or logarithmic functions [11] can be used as well.

3. Fully three-dimensional fiber orientation distribution

In the general case of a distributed fiber reinforced material, the fibers are not aligned in the unique direction $\mathbf{a}_0$ but are spatially oriented according to a symmetric density function $\overline{\rho}(\mathbf{a}) \equiv \overline{\rho}(-\mathbf{a})$ that describes the amount of fibers lying along a certain orientation $\mathbf{a}$. The unit vector $\mathbf{a}$ can be defined in terms of two Eulerian angles $\Theta \in [0, \pi]$ and $\Phi \in [0, 2\pi]$, see Fig. 1(a), as

$$\mathbf{a}(\Theta, \Phi) = \sin\,\Theta\,\cos\,\Phi \mathbf{e}_1 + \sin\,\Theta\,\sin\,\Phi \mathbf{e}_2 + \cos\,\Theta \mathbf{e}_3.$$

Therefore the expression $\overline{\rho}(\mathbf{a})\,\sin\,\Theta\,d\Theta\,d\Phi$ represents the number of fibers whose orientation falls in the range $[(\Theta, \Theta + d\Theta), (\Phi, \Phi + d\Phi)]$. The integral of $\overline{\rho}(\mathbf{a})$ over the unit sphere ω gives

$$\int_\omega \overline{\rho}(\mathbf{a})\, d\omega = \int_0^\pi \int_0^{2\pi} \overline{\rho}(\mathbf{a})\,\sin\,\Theta\, d\Phi\, d\Theta = 4\pi. \tag{3}$$

It follows that the directional second order structure tensor $\mathbf{A} = \mathbf{a} \otimes \mathbf{a}$ is a function of the Eulerian angles, as well as the directional invariant $\bar{I}_4(\mathbf{a}) = \mathbf{A} : \overline{\mathbf{C}}$. For the assumed distribution of fiber orientation, the operator $\langle f \rangle$ provides the average of the function f over the unit sphere:

$$\langle f \rangle = \frac{1}{4\pi} \int_\omega \overline{\rho}(\mathbf{a}) f\, d\omega. \tag{4}$$

Since the deformation tensor $\overline{\mathbf{C}}$ is independent of the Eulerian angles, the average pseudo-invariant $\langle \bar{I}_4 \rangle$ is easily computed as

$$\bar{I}_4^* = \langle \bar{I}_4(\mathbf{a}) \rangle = \frac{1}{4\pi} \int_\omega \overline{\rho}(\mathbf{a}) \bar{I}_4(\mathbf{a})\, d\omega = \frac{1}{4\pi} \int_\omega \overline{\rho}(\mathbf{a}) \mathbf{A}\, d\omega : \overline{\mathbf{C}} = \mathbf{H} : \overline{\mathbf{C}},$$

where we introduce the second order structure tensor $\mathbf{H}$ as

$$\mathbf{H} = \langle \mathbf{A} \rangle.$$

As first observed in [3], in the definition of the average invariant $\bar{I}_4^*$ the fibers under compression cannot be excluded a priori. Therefore, if one of the principal values of $\mathbf{C}$ is less than 1, a fraction of compressed fibers will be included in the average.

The average strain energy density over the unit sphere becomes

$$\Psi^*_{\text{aniso}} = \langle \Psi_{\text{aniso}} \rangle = \frac{1}{4\pi} \int_\omega \overline{\rho}(\mathbf{a}) \Psi_{\text{aniso}}(\bar{I}_4)\, d\omega. \tag{5}$$

Regrettably, in general no close forms of (5) are available, and the hyperelastic approach loses his appeal since the stress cannot be derived analytically. The stress tensor can be obtained only through the numerical calculation of the integral

$$\overline{\mathbf{S}}^*_{\text{aniso}} = \langle \overline{\mathbf{S}}_{\text{aniso}} \rangle = \frac{1}{4\pi} \int_\omega \overline{\rho}(\mathbf{a}) \overline{\mathbf{S}}_{\text{aniso}}(\bar{I}_4)\, d\omega. \tag{6}$$

To alleviate the difficulties inherent to the evaluation of the above expressions, alternative, simplified forms of the strain energy density have been proposed, for example transversally isotropic distributions [7] deriving from the assumption of rotational symmetry of the fiber distribution about a specific referential direction $\mathbf{a}_0$. This circumstance is important in view of biological applications characterized by dominant transversally isotropy. Let us assume here that in the distribution of fibers it is possible to identify a preferential direction $\mathbf{a}_0$. Without loss of generality $\mathbf{a}_0$ can be taken to coincide with the Cartesian basis vector $\mathbf{e}_3$.

As discussed in [19], the generalized structure tensor (GST) model described in [7] can be interpreted as a linearization of the anisotropic strain energy density about the average invariant $\bar{I}_4^*$ (note that $\langle \bar{I}_4 - \bar{I}_4^* \rangle = 0$):

$$\Psi^*_{\text{aniso}} \approx \Psi_{\text{aniso}}(\bar{I}_4^*) + \frac{\partial \Psi_{\text{aniso}}}{\partial \bar{I}_4}\Big|_{\bar{I}_4 = \bar{I}_4^*} \langle \bar{I}_4 - \bar{I}_4^* \rangle = \Psi^0_{\text{aniso}} + \overline{\Psi}^*_{\text{aniso}}. \tag{7}$$

The approximation (7) leads to a handy form that allows for the analytical calculation of the average stress tensor:

$$\overline{\mathbf{S}}^*_{\text{aniso}} = \mathcal{M}\mathbf{H}, \quad \mathcal{M} = 4k_2(\bar{I}_4^* - 1)\overline{\Psi}_{\text{aniso}}(\bar{I}_4^*). \tag{8}$$

Unfortunately the model fails to describe the correct stress distribution for largely dispersed fiber orientations [3]. A better approximation can be obtained by including the second order term (or variance, V) of the strain energy density about the average invariant $\bar{I}_4^*$ [19]:

$$\begin{aligned} \Psi^*_{\text{aniso}} &\approx \Psi_{\text{aniso}}(\bar{I}_4^*) + \frac{1}{2} \frac{\partial^2 \Psi_{\text{aniso}}}{\partial \bar{I}_4^2}\Big|_{\bar{I}_4 = \bar{I}_4^*} \langle (\bar{I}_4 - \bar{I}_4^*)^2 \rangle \\ &= \Psi^0_{\text{aniso}} + \overline{\Psi}^*_{\text{aniso}}(1 + K^* \sigma^2_{\bar{I}_4}), \end{aligned} \tag{9}$$

where we denote

$$K^* = 2k_2^2(\bar{I}_4^* - 1)^2 + k_2$$

and

$$\sigma^2_{\bar{I}_4} = \overline{\mathbf{C}} : \mathbb{H} : \overline{\mathbf{C}} - (\mathbf{H} : \overline{\mathbf{C}})^2.$$

We note that the novel approximation of the strain energy density introduces the average fourth order tensor $\mathbb{H} = \langle \mathbf{A} \otimes \mathbf{A} \rangle$.

Through (2), the second order approximation of the average anisotropic strain energy density (9) leads to the explicit form of the second Piola–Kirchhoff stress

$$\overline{\mathbf{S}}^*_{\text{aniso}} = \alpha \mathbf{H} + \beta \mathbb{H} : \overline{\mathbf{C}}, \tag{10}$$

and of the associated tangent stiffness

$$\overline{\mathbb{C}}^*_{\text{aniso}} = \langle \overline{\mathbb{C}}_{\text{aniso}} \rangle = J^{-4/3}(\gamma \mathbf{H} \otimes \mathbf{H} + \delta \mathbf{H} \otimes \mathbb{H} : \overline{\mathbf{C}} + 2\beta \mathbb{H}), \tag{11}$$

where

$$\alpha = \overline{\Psi}^*_{\text{aniso}} \sum_{j=0}^{3} a_j \bar{I}_4^{*j}, \quad \beta = \overline{\Psi}^*_{\text{aniso}} \sum_{j=0}^{2} b_j \bar{I}_4^{*j}, \tag{12}$$

$$\gamma = \overline{\Psi}^*_{\text{aniso}} \sum_{j=0}^{4} c_j \bar{I}_4^{*j}, \quad \delta = \overline{\Psi}^*_{\text{aniso}} \sum_{j=0}^{3} d_j \bar{I}_4^{*j}. \tag{13}$$

Explicit formulae for coefficients a_j, b_j, c_j, d_j are reported in Appendix A.

3.1. Covariance stress tensors

The fourth order covariance tensor of the second Piola–Kirchhoff stress tensor, or the covariance stress tensor, is defined as

$$\overline{\mathbb{R}}_{\text{aniso}} = \langle \overline{\mathbf{S}}_{\text{aniso}} \otimes \overline{\mathbf{S}}_{\text{aniso}} \rangle - \langle \overline{\mathbf{S}}_{\text{aniso}} \rangle \otimes \langle \overline{\mathbf{S}}_{\text{aniso}} \rangle.$$

Recalling (8), we can evaluate a linear approximation of the average stress and the average stress dyadic product as

$$\langle \overline{\mathbf{S}}_{\text{aniso}} \rangle = \mathcal{M}\,\mathbf{H}, \quad \langle \overline{\mathbf{S}}_{\text{aniso}} \otimes \overline{\mathbf{S}}_{\text{aniso}} \rangle = \mathcal{M}^2\,\mathbb{H}.$$

Therefore $\overline{\mathbb{R}}_{\text{aniso}}$ takes the form

$$\overline{\mathbb{R}}_{\text{aniso}} = \mathcal{M}^2(\mathbb{H} - \mathbf{H} \otimes \mathbf{H}), \tag{14}$$

or, in index notation

$$\overline{R}_{IJHK} = \mathcal{M}^2(H_{IJHK} - H_{IJ}H_{HK}).$$

It is worth noting that the covariance tensor of the directional second order structure tensor $\mathbf{A}$ is given by

$$\mathbb{R}_{\mathbf{A}} = \mathbb{H} - \mathbf{H} \otimes \mathbf{H},$$

therefore the linear approximation of the covariance stress tensor (14) becomes

$$\overline{\mathbb{R}}^{\mathrm{GST}}_{\mathrm{aniso}} = \mathcal{M}^2 \mathbb{R}_{\mathbf{A}}. \tag{15}$$

Alternatively, a second order approximation of the covariance stress tensor can be derived from the expression of the average stress tensor (8), leading to

$$\overline{\mathbb{R}}^{V}_{\mathrm{aniso}} = \alpha^2 \mathbb{R}_{\mathbf{A}}, \tag{16}$$

where α is defined in Eq. $(12)_1$.

We recall that the relation between the Cauchy stress tensor and the second Piola–Kirchhoff stress tensor is

$$\boldsymbol{\sigma} = J^{-1}\mathbf{F}\mathbf{S}\mathbf{F}^T.$$

The isochoric anisotropic Cauchy stress $\overline{\boldsymbol{\sigma}}_{\mathrm{aniso}}$ is related to the anisotropic second Piola–Kirchhoff stress $\overline{\mathbf{S}}_{\mathrm{aniso}}$ in the form [10]

$$\overline{\boldsymbol{\sigma}}_{\mathrm{aniso}} = J^{-1}\overline{\mathbf{F}}(\mathbb{P} : \overline{\mathbf{S}}_{\mathrm{aniso}})\overline{\mathbf{F}}^T = J^{-1}\mathcal{M}\overline{\mathbf{F}}(\mathbb{P} : \mathbf{A})\overline{\mathbf{F}}^T,$$

where $\mathbb{P}$ is the fourth order projection tensor. It follows that the average Cauchy stress is

$$\langle\overline{\boldsymbol{\sigma}}_{\mathrm{aniso}}\rangle = J^{-1}\mathcal{M}\overline{\mathbf{F}}(\mathbb{P} : \mathbf{H})\overline{\mathbf{F}}^T,$$

or, in components

$$(\langle\overline{\boldsymbol{\sigma}}_{\mathrm{aniso}}\rangle)_{ab} = J^{-1}\mathcal{M}\overline{F}_{aA}\overline{F}_{bB}\mathcal{P}_{ABIJ}H_{IJ},$$

where $\mathcal{P}_{ABIJ}$ are the components of $\mathbb{P}$. Therefore, the Cauchy covariance stress tensor is defined as

$$\overline{\mathbb{R}}^{\sigma}_{\mathrm{aniso}} = \langle\overline{\boldsymbol{\sigma}}_{\mathrm{aniso}} \otimes \overline{\boldsymbol{\sigma}}_{\mathrm{aniso}}\rangle - \langle\overline{\boldsymbol{\sigma}}_{\mathrm{aniso}}\rangle \otimes \langle\overline{\boldsymbol{\sigma}}_{\mathrm{aniso}}\rangle$$

or, in components,

$$(\overline{\mathbb{R}}^{\sigma}_{\mathrm{aniso}})_{abcd} = J^{-2}\overline{F}_{aA}\overline{F}_{bB}\overline{F}_{cC}\overline{F}_{dD}\mathcal{P}_{ABIJ}\overline{R}_{IJHK}\mathcal{P}_{CDHK}.$$

3.2. Rotation of the reference configuration

The previous definition of the fourth order tensor $\mathbb{H}$ refers to the particular orientation of the mean direction of the fibers $\mathbf{e}_3$. In order to apply the model to a generic main orientation $\mathbf{a}_0$, the fourth order tensor $\mathbb{H}$ has to be rotated, for example according to the following method. The two unit vectors $\mathbf{a}_0$ and $\mathbf{e}_3$ are separated by the angle θ

$$\cos\,\theta = \mathbf{e}_3 \cdot \mathbf{a}_0,$$

and the two vectors define a plane of normal $\mathbf{n}$

$$\mathbf{n} = \frac{\mathbf{e}_3 \times \mathbf{a}_0}{|\mathbf{e}_3 \times \mathbf{a}_0|}.$$

A rotation of amplitude θ about the vector $\mathbf{n}$, of components n_I, is obtained by using the following matrix $\mathbf{R} \in SO(3)$

$$\mathbf{R} = \begin{bmatrix} c+n_1^2(1-c) & n_3 s+n_1 n_2(1-c) & -n_2 s+n_3 n_1(1-c) \\ -n_3 s+n_1 n_2(1-c) & c+n_2^2(1-c) & n_1 s+n_2 n_3(1-c) \\ n_2 s+n_3 n_1(1-c) & -n_1 s+n_2 n_3(1-c) & c+n_3^2(1-c) \end{bmatrix}$$

with $s = \sin\,\theta$ and $c = \cos\,\theta$. If R_{IJ} denotes the component of $\mathbf{R}$, the rotation of $\mathbb{H}$ is performed according to the following rule:

$$H_{IJHK} = H_{ABCD}R_{AI}R_{BJ}R_{CH}R_{DK}.$$

3.3. Transversely isotropic material

A commonly adopted distribution of fibers related to a transversely isotropic material is the π-periodic normalized von Mises distribution [24], centered at $\Theta = 0$. Therefore we assume

$$\overline{\rho}(\Theta) = \frac{1}{2\pi I}\exp(b\,\cos\,2\Theta), \tag{17}$$

where

$$I = \frac{1}{\pi}\int_0^{\pi} \exp(b\,\cos\,2\Theta)\,d\Theta.$$

It follows that the density function becomes independent of Φ, $\overline{\rho}(\mathbf{a}) \equiv \rho(\Theta)$, and the normalization condition (3) reduces to

$$\int_0^{\pi} \rho(\Theta)\,\sin\,\Theta\,d\Theta = 2.$$

The assumption of rotational symmetry leads to the explicit evaluation of the average second order structure tensor $\mathbf{H}$

$$\mathbf{H} = \langle\mathbf{A}\rangle = \begin{bmatrix} \kappa & 0 & 0 \\ 0 & \kappa & 0 \\ 0 & 0 & 1-2\kappa \end{bmatrix},$$

in terms of the unique constant κ [7]:

$$\kappa = \frac{1}{4}\int_0^{\pi} \rho(\Theta)\,\sin^3\,\Theta\,d\Theta. \tag{18}$$

The novel approximation of the strain energy density requires the average fourth order tensor $\mathbb{H} = \langle\mathbf{A} \otimes \mathbf{A}\rangle$ with non-zero coefficients:

$$\begin{aligned}
&H_{1111} = H_{2222} = 3\widehat{\kappa},\\
&H_{3333} = 1-4\kappa+8\widehat{\kappa},\\
&H_{1122} = H_{2211} = H_{1212} = H_{2121} = H_{1221} = H_{2112} = \widehat{\kappa},\\
&H_{2233} = H_{3322} = H_{2323} = H_{3232} = H_{2332} = H_{3223} = \kappa-4\widehat{\kappa},\\
&H_{3311} = H_{1133} = H_{3131} = H_{1313} = H_{3113} = H_{1331} = \kappa-4\widehat{\kappa},
\end{aligned}$$

where $\widehat{\kappa}$ is given by

$$\widehat{\kappa} = \frac{1}{16}\int_0^{\pi} \rho(\Theta)\,\sin^5\,\Theta\,d\Theta. \tag{19}$$

The relation between the dispersion parameters κ, $\widehat{\kappa}$ and the concentration parameter b of the von Mises distribution is shown in Fig. 2. Note that the von Mises distribution is defined for $b > 0$, therefore the ranges of the two parameters are $\kappa \in [0, 1/3]$ and $\widehat{\kappa} \in [0, 1/15]$. Fig. 2 shows that for $b > 4$ the parameter $\widehat{\kappa}$ becomes very small and its contribution vanishes. Thus, the model recovers the linearized distributed model proposed in [7]. This means that the largest differences are observed in materials characterized by rather large dispersion and little alignment of the fibers.

Within the von Mises distribution, the non-zero elements of the covariance tensor $\mathbb{R}_{\mathbf{A}}$ are

$$\begin{aligned}
&\overline{R}_{1111} = \overline{R}_{2222} = 3\widehat{\kappa}-\kappa^2\\
&\overline{R}_{3333} = 8\widehat{\kappa}-4\kappa^2\\
&\overline{R}_{1212} = \overline{R}_{2121} = \overline{R}_{1221} = \overline{R}_{2112} = \widehat{\kappa}
\end{aligned}$$

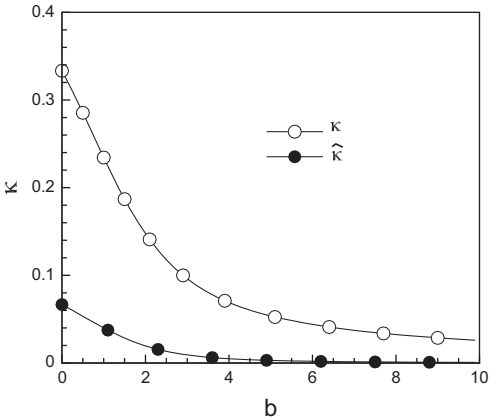

Fig. 2. Dependence of the dispersion parameters κ, Eq. (18), and $\widehat{\kappa}$, Eq. (19), on the concentration parameter b, for the three-dimensional normalized von Mises distribution, see Eq. (17).

$$\overline{R}_{1122}=\overline{R}_{2211}=\widehat{\kappa}-\kappa^2$$
$$\overline{R}_{2323}=\overline{R}_{3232}=\overline{R}_{2332}=\overline{R}_{3223}=-4\widehat{\kappa}+\kappa$$
$$\overline{R}_{2233}=\overline{R}_{3322}=-4\widehat{\kappa}+2\kappa^2$$
$$\overline{R}_{3131}=\overline{R}_{1313}=\overline{R}_{3113}=\overline{R}_{1331}=-4\widehat{\kappa}+\kappa$$
$$\overline{R}_{3311}=\overline{R}_{1133}=-4\widehat{\kappa}+2\kappa^2.$$

4. Planar fiber distribution

A planar formulation may be obtained by specializing the distribution density $\overline{\rho}(\mathbf{a})$. As remarked in [24], although accounting for a planar distribution of the fibers, the structural tensor is a true three-dimensional tensor and the derived stresses are three-dimensional.

We begin by referring to a planar distribution lying on the plane normal to the direction $\mathbf{e}_1$ where $\Phi=\pi/2$ and, for the obvious symmetry, we limit $\Theta\in[-\pi/2,\pi/2]$. We assume independence of the angle Φ and write

$$\overline{\rho}(\mathbf{a})=\rho(\Theta). \tag{20}$$

The quantity $\rho(\Theta)\,d\Theta$ represents the amount of fibers lying on the direction Θ, see Fig. 1(b). The normalization condition in the half circle becomes

$$\frac{1}{\pi}\int_{-\pi/2}^{\pi/2}\rho(\Theta)\,d\Theta=1.$$

The average definition (4) in two-dimensions becomes

$$\langle f\rangle=\frac{1}{\pi}\int_{-\pi/2}^{\pi/2}\rho(\Theta)f\,d\Theta. \tag{21}$$

Now we account for a π-periodic distribution that depends only on the angle Θ. With no loss of generality, we assume that the mean orientation of the fibers is in the direction $\mathbf{a}_0=\mathbf{e}_3$. According to the definition (21), it is possible to derive the average structure tensor $\mathbf{H}^{\rm pl}$ in explicit form as

$$\mathbf{H}^{\rm pl}=\begin{bmatrix}0&0&0\\0&\kappa^{\rm pl}&0\\0&0&1-\kappa^{\rm pl}\end{bmatrix},$$

where $\kappa^{\rm pl}$ is proportional to the dispersion factor introduced in [24]:

$$\kappa^{\rm pl}=\frac{1}{\pi}\int_{-\pi/2}^{\pi/2}\rho(\Theta)\,\sin^2\Theta\,d\Theta. \tag{22}$$

The non-zero terms of the average fourth order tensor $\mathbb{H}^{\rm pl}$ follow in explicit form as

$$H^{\rm pl}_{2222}=\widehat{\kappa}^{\rm pl},$$
$$H^{\rm pl}_{3322}=H^{\rm pl}_{2233}=H^{\rm pl}_{3232}=H^{\rm pl}_{2323}=H^{\rm pl}_{3223}=H^{\rm pl}_{2332}=\kappa^{\rm pl}-\widehat{\kappa}^{\rm pl},$$
$$H^{\rm pl}_{3333}=1-2\kappa^{\rm pl}+\widehat{\kappa}^{\rm pl},$$

where $\widehat{\kappa}^{\rm pl}$ is

$$\widehat{\kappa}^{\rm pl}=\frac{1}{\pi}\int_{-\pi/2}^{\pi/2}\rho(\Theta)\,\sin^4\Theta\,d\Theta. \tag{23}$$

The non-zero components of the planar covariance tensor $\mathbb{R}^{\rm pl}_{\mathbf{A}}$ are

$$\overline{R}^{\rm pl}_{2222}=\overline{R}^{\rm pl}_{3333}=\widehat{\kappa}^{\rm pl}-{\kappa^{\rm pl}}^2$$
$$\overline{R}^{\rm pl}_{3232}=\overline{R}^{\rm pl}_{2323}=\overline{R}^{\rm pl}_{3223}=\overline{R}^{\rm pl}_{2332}=\kappa^{\rm pl}-\widehat{\kappa}^{\rm pl}$$
$$\overline{R}^{\rm pl}_{3322}=\overline{R}^{\rm pl}_{2233}={\kappa^{\rm pl}}^2-\widehat{\kappa}^{\rm pl}.$$

If the normal $\mathbf{n}$ to the fiber plane does not coincide with $\mathbf{e}_1$, i.e. $\mathbf{a}_0\neq\mathbf{e}_3$, the tensors $\mathbf{H}^{\rm pl}$ and $\mathbb{H}^{\rm pl}$ must be rotated. To this aim, we introduce the unit vector $\mathbf{b}$ forming an orthonormal basis with $\mathbf{n}$ and $\mathbf{a}_0$:

$$\mathbf{b}=\frac{\mathbf{a}_0\times\mathbf{n}}{|\mathbf{a}_0\times\mathbf{n}|}. \tag{24}$$

Thus, the rotation matrix $\mathbf{R}^{\rm pl}\in SO(3)$ is defined as

$$\mathbf{R}^{\rm pl}=\begin{bmatrix}n_1&b_1&a_{01}\\n_2&b_2&a_{02}\\n_3&b_3&a_{03}\end{bmatrix},$$

leading to

$$H^{\rm pl}_{IJ}=H^{\rm pl}_{AB}R^{\rm pl}_{AI}R^{\rm pl}_{JB}.$$

and

$$H^{\rm pl}_{IJHK}=H^{\rm pl}_{ABCD}R^{\rm pl}_{AI}R^{\rm pl}_{BJ}R^{\rm pl}_{CH}R^{\rm pl}_{DK}.$$

4.1. von Mises distribution

In view of numerical tests we consider the π-periodic normalized von Mises distribution, centered at $\Theta=0$. Therefore we assume

$$\rho(\Theta)=\frac{1}{\pi I^0}\exp(b\,\cos 2\Theta), \tag{25}$$

where, in order to satisfy (21), the normalization coefficient I^0 becomes

$$I^0=\frac{1}{\pi}\int_{-\pi/2}^{\pi/2}\exp(b\,\cos\,2\Theta)\,d\Theta.$$

The relation between the dispersion parameters $\kappa^{\rm pl}$, $\widehat{\kappa}^{\rm pl}$ and the concentration parameter b is shown in Fig. 3. The range of the two values is $\kappa^{\rm pl}\in[0,1/8\pi]$, $\widehat{\kappa}^{\rm pl}\in[0,1/16\pi]$. Fig. 3 shows that for $b>4$ the parameter $\widehat{\kappa}^{\rm pl}$ becomes very small, and its contribution vanishes. Such a behavior is similar to the one observed for the three-dimensional formulation, Fig. 2, even though the two coefficients assume higher values for small b. For the von Mises distribution the expression of the strain energy density becomes

$$\Psi^{*\rm pl}_{\rm aniso}=\frac{1}{\pi}\int_{-\pi/2}^{\pi/2}\rho(\Theta)\Psi_{\rm aniso}(\bar{I}_4)\,d\Theta,$$

where $\bar{I}_4$ is a function of the sole angle $\Theta\in[-\pi/2,\pi/2]$. The expression of the stress is

$$\overline{\mathbf{S}}^{*\rm pl}_{\rm aniso}=\frac{1}{\pi}\int_{-\pi/2}^{\pi/2}\rho(\Theta)\overline{\mathbf{S}}_{\rm aniso}\,d\Theta, \tag{26}$$

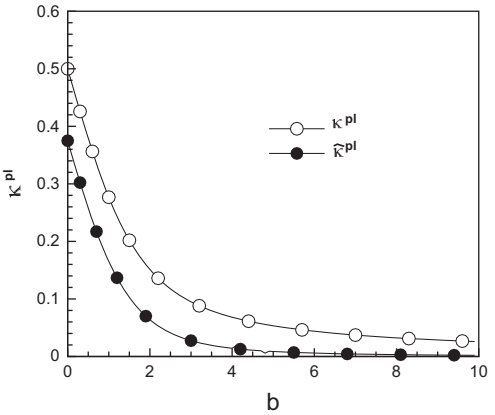

Fig. 3. Dependence of the dispersion parameters $\kappa^{\rm pl}$, Eq. (22), and $\widehat{\kappa}^{\rm pl}$, Eq. (23), on the concentration b, for the two-dimensional normalized von Mises distribution, see Eq. (25).

where $\bar{\mathbf{S}}_{\text{aniso}}$ is defined in $(2)_2$. For the particular expression of the fiber strain energy density Ψ_{aniso} chosen here, the second order approximation of the stress and stiffness tensors will preserve the structure observed in (10) and (11), where the tensors $\mathbf{H}$ and $\mathbb{H}$ are replaced by $\mathbf{H}^{\text{pl}}$ and $\mathbb{H}^{\text{pl}}$ respectively.

5. Numerical tests

We begin by considering the uniaxial behavior of the proposed models. Since we are focusing on the anisotropic response, in the following calculation we do not account for the volumetric and the

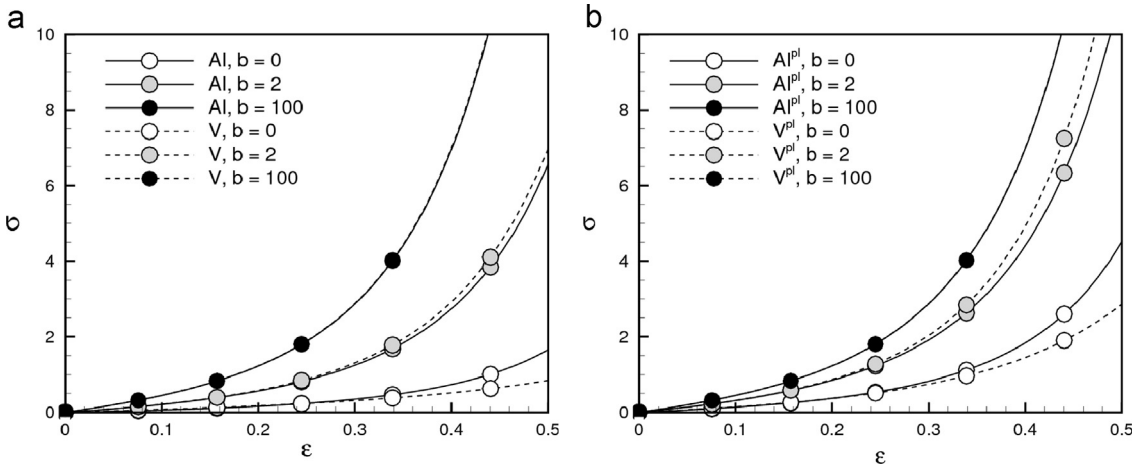

Fig. 4. Uniaxial true stress–true strain curves, stress in MPa. Solid lines show the exactly integrated solution. Broken lines show the second order approximation. Black circles refer to the case $b=100$, or strongly aligned fibers. Gray circles describe a case with average dispersion $b=2$. White circles refer to the fully isotropic distribution, $b=0$. (a) Three-dimensional response. (b) Two-dimensional response.

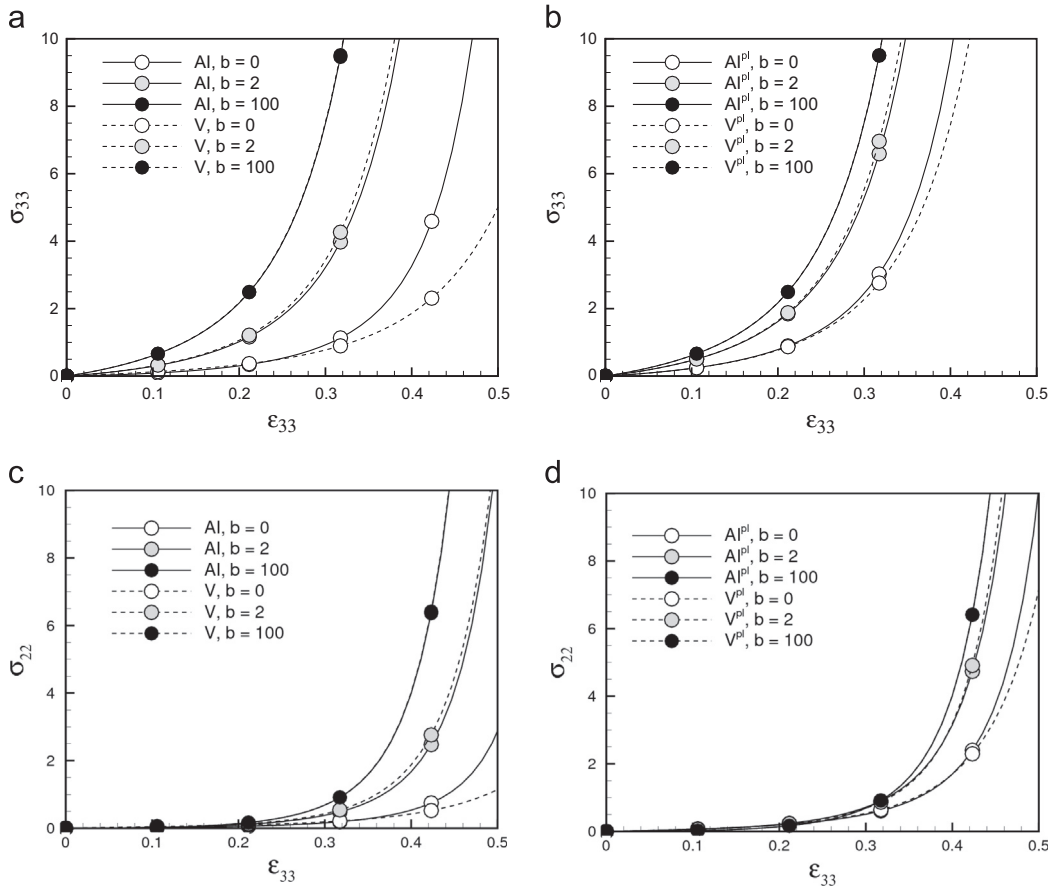

Fig. 5. Biaxial true stress–true strain curves, stress in MPa. Solid lines show the exactly integrated solution. Broken lines show the second order approximation. Black circles refer to the case $b=100$, or strongly aligned fibers. Gray circles describe a case with average dispersion $b=2$. White circles refer to the fully isotropic distribution, $b=0$. Maximum stretches $\lambda_2 = 1.0$, $\lambda_3 = 1.8$ ($\lambda_1 = 1/1.8$). (a) Three-dimensional response, mean fiber direction. (b) Two-dimensional response, mean fiber direction. (c) Three-dimensional response, direction normal to the fibers. (b) Two-dimensional response, direction normal to the fibers.

isotropic part of the strain energy. The parameters of the model are set to the unit $k_1 = 1$ MPa and $k_2 = 1$. The concentration parameter b of the von Mises distribution will be modified in order to describe different fiber dispersions. In the following plots, we refer to the three-dimensional and two-dimensional models with exact angle integration (i.e., where the stress is computed according to definitions (6)–(26)), as AI and AI^{pl} respectively; to the three-dimensional and two-dimensional second order

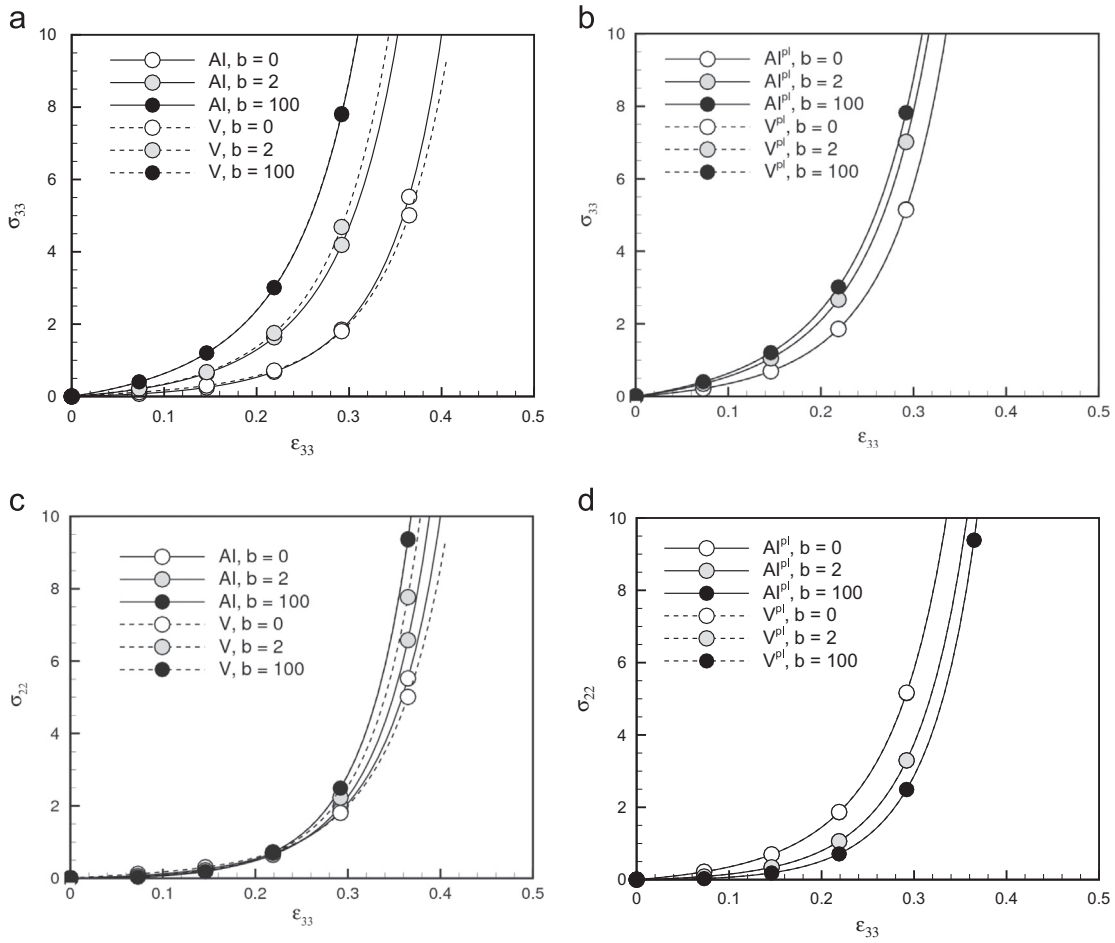

Fig. 6. Equibiaxial true stress–true strain curves, stress in MPa. Solid lines show the exactly integrated solution. Broken lines show the second order approximation. Black circles refer to the case $b=100$, or strongly aligned fibers. Gray circles describe a case with average dispersion $b=2$. White circles refer to the fully isotropic distribution, $b=0$. Maximum stretches $\lambda_2 = \lambda_3 = 1.5$. (a) Three-dimensional response, mean fiber direction. (b) Two-dimensional response, mean fiber direction. (c) Three-dimensional response, direction normal to the fibers. (b) Two-dimensional response, direction normal to the fibers.

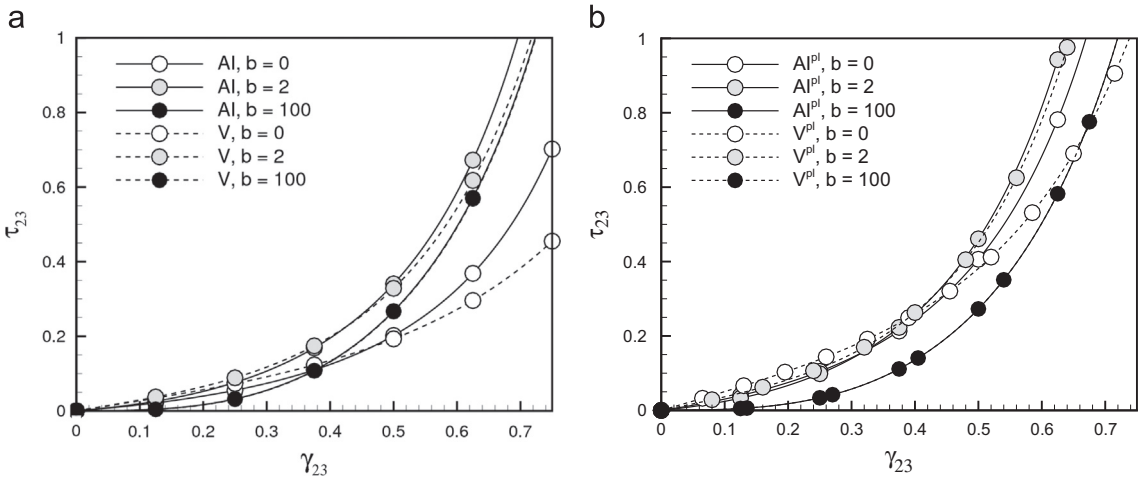

Fig. 7. Shear stress–strain curves, stress in MPa. Solid lines show the exactly integrated solution. Broken lines show the second order approximation. Black circles refer to the case $b=100$, or strongly aligned fibers. Gray circles describe a case with average dispersion $b=2$. White circles refer to the fully isotropic distribution, $b=0$. (a) Three-dimensional response. (b) Two-dimensional response.

approximation models as V and V^{pl} respectively; and to the three-dimensional and two-dimensional first order approximation models as GST and GST^{pl}, respectively.

Fig. 4 shows uniaxial stress–strain curves where the AI and AI^{pl} stresses are compared with the V and V^{pl} stresses, for the three- and two-dimensional cases respectively. The figures show that the V and V^{pl} approximations are good, also in the case of dispersed fibers. It clearly appears that the two-dimensional model is characterized by a larger stiffness, due to the fact that the fibers are distributed on a plane and not over the unit sphere. It is also evident that, for the strongly aligned fiber case, the three- and two-dimensional models provide the same response.

Fig. 5 shows stress–strain curves for biaxial deformations, up to $\lambda_3 = 1.8, \lambda_2 = 1.0, \lambda_1 = 1/1.8$. The main direction of the fibers is 3.

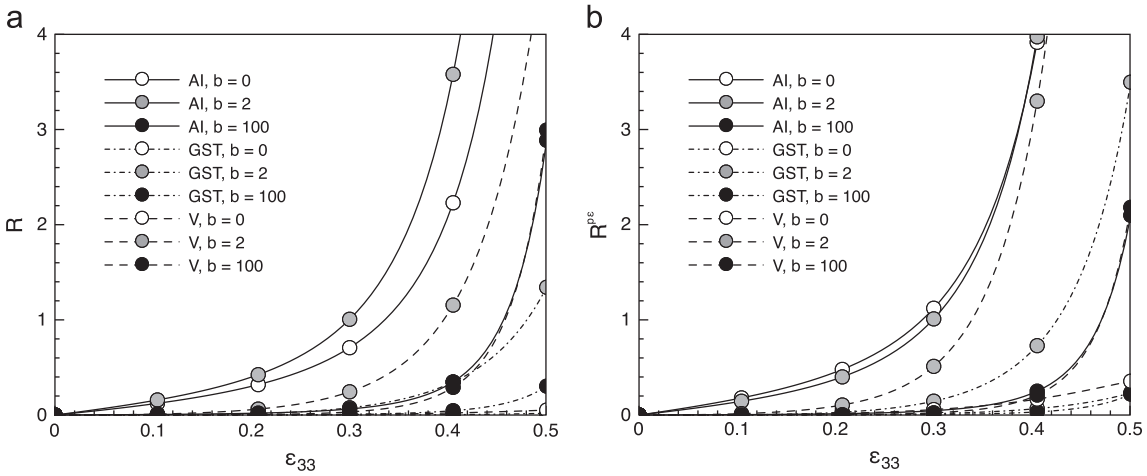

Fig. 8. Covariance stress component R_{3333} (MPa^2) versus strain in uniaxial loading. Solid lines show the exactly integrated solution. Dash-dot lines show the first order approximation. Broken lines show the second order approximation. Black circles refer to the case $b=100$, or strongly aligned fibers. Gray circles describe a case with average dispersion $b=2$. White circles refer to the fully isotropic distribution, $b=0$. (a) Three-dimensional response. (b) Two-dimensional response.

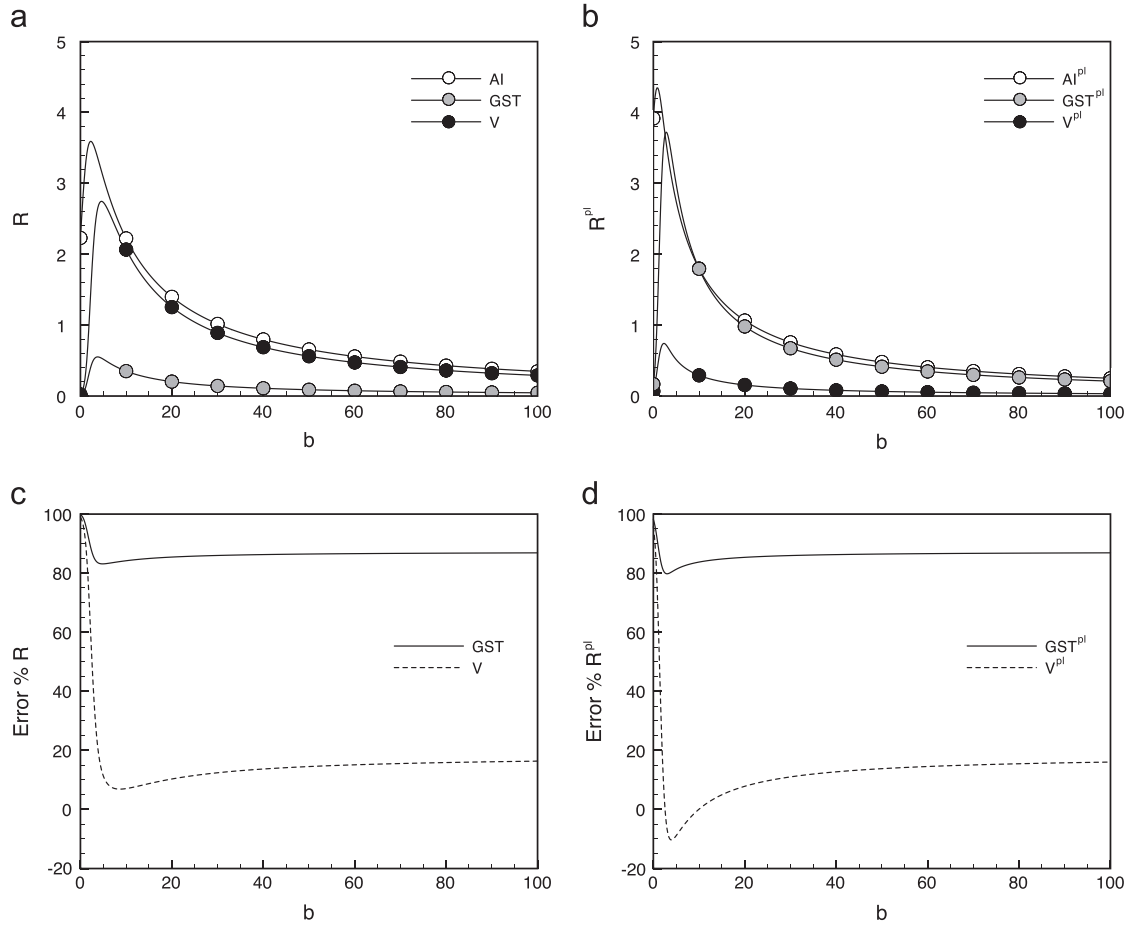

Fig. 9. Covariance stress component R_{3333} (MPa^2) versus the concentration coefficient b. White circles refer to the case of exact integration, gray circles refer to the case of first order approximation and black circles refer to the second order approximation. (a) Three-dimensional case, absolute values. (b) Two-dimensional case, absolute values. (c) Three-dimensional case, % error. (c) Two-dimensional case, % error.

The exactly integrated stresses, in the direction of the applied stretches, are compared with the second order approximations, for the three- and two-dimensional cases, respectively.

Fig. 6 shows similar stress–strain curves for equibiaxial deformations, up to $\lambda_2 = \lambda_3 = 1.5$, and $\lambda_1 = 1/1.5^2$. Note that the model V^{pl} provides the exact response for any value of b. This can be easily understood, since under equibiaxial loading all the planar fibers are equally activated in tension. The error is still limited for the V model.

Fig. 7 shows stress–strain curves for the case of pure shear deformation in the plane of the fibers 2–3, up to $\gamma_{23} = 0.7$. Also in this case, the main direction of the fibers is 3, and the exact solutions are compared with the second order approximations, for the three- and two-dimensional cases respectively. Both V and V^{pl} models are able to capture the shear response of the exactly integrated model, with maximum discrepancy for the fully distributed fiber case.

Fig. 8 plots the uniaxial covariance stress. The square root of the R_{3333} component of the AI and AI^{pl} covariance stress is compared to the same quantity for the GST, GST^{pl}, V and V^{pl} covariance stress, for the three-dimensional case, Fig. 8(a), and the two-dimensional case, Fig. 8(b). The plots show that the V and V^{pl} approximations are much better than the GST and GST^{pl} ones. It clearly appears that the two-dimensional model is characterized in general by a better approximation, due to the fact that the fibers are distributed on a plane and not over the unit sphere. It is also evident that, for the strongly aligned fiber case, the three- and two-dimensional models provide the same response.

Fig. 9 visualizes the uniaxial covariance stress versus the concentration parameter b. The square root of the covariance stress component R_{3333} AI and AI^{pl} is compared with the same component for the GST, GST^{pl}, V and V^{pl}, in the three-dimensional case, Fig. 9(a), and two-dimensional case, Fig. 9(b), respectively. Fig. 9(c) and (d) plots then percentage error with respect to the exact integration. It is worth noting that the covariance stress reaches a maximum value for $b \approx 2$.

6. Conclusions

We present a study on the mechanical response of hyperelastic fiber reinforced models with statistical distribution of the fiber orientation. As starting point, we refer to a recent contribution by Pandolfi and Vasta [19] that introduced the concept of the second order (or variance) approximation. The model describes the features of the fiber distribution by means of the average and the variance of the fourth pseudo-invariant $\bar{I}_4$. As demonstrated in [19], in the particular case of transversally isotropic materials (e.g. we choose the von Mises distribution) the variance model approximates the exactly integrated model in a better way than alternative models accounting exclusively for the average pseudo-invariant $\bar{I}_4^*$. The better behavior has been demonstrated for a few significant loading conditions, i.e., uniaxial, biaxial and pure shear.

For the second order approximation model, new studies reported in the present contribution discuss the concept of covariance stress tensors and the specialization to a planar fiber distribution.

For a more exhaustive probabilistic characterization of the response of fiber distributed materials, the knowledge of the second order statistics is mandatory. To this end, we studied the covariance stress tensor for the second Piola–Kirchhoff and Cauchy stresses. We prove that the covariance stress tensor is proportional to the covariance stress tensor of the directional second order tensor $\mathbf{A}$ that characterizes the second order approximation elasticity tensor. Furthermore, two approximated explicit expressions of the covariance stress tensors are derived.

Second, we specialize the model for two-dimensional distributions of the fiber orientation, in order to be able to describe materials frequently observed in biology and biomechanics. We follow the path of reasoning found in [24], and describe a second order approximation material model instead of the linearized model presented in [24]. The two-dimensional model can be formulated in analytical form for any two-dimensional distribution of the fiber orientation. Note that only the fiber distribution is two-dimensional, while the material model is fully three-dimensional, to be used within three-dimensional solids and not restricted to dimension-reduced structures, such as plates or shells.

Additionally, in view of the implementation of the model in numerical codes, we illustrate how to perform the rotation of the anisotropic stress and elasticity tensors. The rotation allows us to apply the constitutive model to any distribution characterized by the main orientation of the fibers different from $\mathbf{e}_3$, for which all the analytical expressions here reported have been derived.

Numerical tests are carried on for the sole isochoric component of the material model, i.e., by excluding the contribution of the volumetric deformation and the isochoric–isotropic behavior of the matrix. For the particular case of the von Mises distribution of the fiber orientation, where the exactly integrated numerical solutions can be easily computed, we simulate uniaxial, biaxial, equi-biaxial and shear tests in the three-dimensional and two-dimensional settings.

The results demonstrate that the second order approximation provides accurate values of the mechanical response of material models with statistically distributed orientation of the fibers. The two-dimensional model is particularly interesting for loadings in uniaxial, equi-biaxial, and shear conditions.

Acknowledgments

AP wishes to thank the financial support from the Italian MIUR (Grant no. PRIN #200959L72B 004) through the 2010 grant "Mathematics and mechanics of the adaptive microstructure of soft biological tissues". AG wishes to thank the financial support from the Italian GNFM, INdAM Young Researcher 2013 grant (Grant no. U2013/000123).

Appendix A

Coefficients:

$$
\begin{aligned}
a_0 &= -4k_2 - 8\sigma_{\bar{I}_4}^2 k_2^3 - 12\sigma_{\bar{I}_4}^2 k_2^2 \\
a_1 &= 24\sigma_{\bar{I}_4}^2 k_2^3 + 12\sigma_{\bar{I}_4}^2 k_2^2 - 8k_2^2 \\
a_2 &= 16k_2^2 - 24\sigma_{\bar{I}_4}^2 k_2^3 \\
a_3 &= 8\sigma_{\bar{I}_4}^2 k_2^3 - 8k_2^2 \\
b_0 &= 4k_2 + 8k_2^2 \\
b_1 &= -16k_2^2 \\
b_2 &= 8k_2^2 \\
c_0 &= \sigma_{\bar{I}_4}^2 (32k_2^4 + 96k_2^3 + 24k_2^2) \\
c_1 &= 96k_2^2 + 64k_2^3 - 192\sigma_{\bar{I}_4}^2 k_2^3 - 128\sigma_{\bar{I}_4}^2 k_2^4 \\
c_2 &= 192\sigma_{\bar{I}_4}^2 k_2^4 + 96\sigma_{\bar{I}_4}^2 k_2^3 - 192k_2^3 - 96k_2^2 \\
c_3 &= 1928k_2^3 - 128\sigma_{\bar{I}_4}^2 k_2^4 \\
c_4 &= 328\sigma_{\bar{I}_4}^2 k_2^4 - 64k_2^3 \\
d_0 &= 64k_2^3 - 96k_2^2 \\
d_1 &= 192k_2^3 + 96k_2^2 \\
d_2 &= -192k_2^3 \\
d_3 &= 64k_2^3
\end{aligned}
\tag{27}
$$

References

[1] Alastrué V, Martinez MA, Menzel A, Doblaré M. On the use of non-linear transformations for the evaluation of anisotropic rotationally symmetric directional integrals. Application to the stress analysis in fibred soft tissues. Int J Numer Methods Eng 2010;79(4):474–504.

[2] Boote C, Dennis S, Newton RH, Puri H, Meek KH. Collagen fibrils appear more closely packed in the prepupillary cornea: optical and biomechanical implications. Invest Ophthalmol Vis Sci 2003;44(7):2941–2948.

[3] Cortes DH, Lake SP, Kadlowec JA, Soslowsky LJ, Elliott DM. Characterizing the mechanical contribution of fiber angular distribution in connective tissue: comparison of two modeling approaches. Biomech Model Mechanobiol 2010;11:651–658.

[4] Daxer A, Fratzl P. Collagen fibril orientation in the human corneal stroma and its implication in keratoconus. Invest Ophthalmol Vis Sci 1997;38:121–129.

[5] Ehret AE, Itskov M. A polyconvex hyperelastic model for fiber-reinforced materials in application to soft tissues. J Mater Sci 2007;42:8853–8863.

[6] Federico S, Gasser TC. Nonlinear elasticity of biological tissues with statistical fibre orientation. J R Soc Interface 2010;7:955–966.

[7] Gasser TC, Ogden RW, Holzapfel GA. Hyperelastic modelling of arterial layers with distributed collagen fibre orientations. J R Soc Interface 2006;3:15–35.

[8] Gizzi A, Cherubini C, Pomella N, Persichetti P, Vasta M, Filippi S. Computational modeling and stress analysis of columellar biomechanics. J Mech Behav Biomed Mater 2012;15:46–58.

[9] Holzapfel GA. Nonlinear solid mechanics: a continuum approach for engineering. New York: John Wiley & Sons; 2000.

[10] Holzapfel GA, Gasser TC, Ogden RW. A new constitutive framework for arterial wall mechanics and a comparative study of material models. J Elast 2000;61:1–48.

[11] Horgan CO, Saccomandi G. A new constitutive theory for fiber-reinforced incompressible nonlinearly elastic solids. J Mech Phys Solids 2005;53(9):1985–2015.

[12] Humphrey JD, Strumpf RK, Yin FCP. Determination of a constitutive relation for passive myocardium: I. A new functional form. J Biomech Eng 1990;112(3):333–339.

[13] Kroon M, Holzapfel GA. A new constitutive model for multi-layered collagenous tissues. J Biomech 2008;41:2766–2771.

[14] Lanir Y. A structural theory for the homogeneous biaxial stress–strain relationship in flat collagenous tissues. J Biomech 1979;12:423–436.

[15] Meek KM, Blamires T, Elliott GF, Nave C. The organisation of collagen fibrils in the human corneal stroma: a synchrotron X-ray diffraction study. Curr Eye Res 1987;6:841–846.

[16] Meek KM, Newton RH. Organization of collagen fibrils in the corneal stroma in relation to mechanical properties and surgical practice. J Refract Surg 1999;15:695–699.

[17] Ogden RW, Saccomandi G. Introducing mesoscopic information into constitutive equations for arterial walls. Biomech Model Mechanobiol 2007;6:333–344.

[18] Pandolfi A, Manganiello F. A model for the human cornea: constitutive formulation and numerical analysis. Biomech Model Mechanobiol 2006;5:237–246.

[19] Pandolfi A, Vasta M. Fiber distributed hyperelastic modeling of biological tissues. Mech Mater 2012;44:151–162.

[20] Petsche SJ, Pinsky PM. The role of 3-d collagen organization in stromal elasticity: a model based on X-ray diffraction data and second harmonic-generated images. Biomech Model Mechanobiol 2013;12:1101–1113.

[21] Raghupathy R, Barocas VH. A closed-form structural model of planar fibrous tissue mechanics. J Biomech 2009;42:1424–1428.

[22] Spencer AJM. Deformations of fibre-reinforced materials. Oxford: Oxford Science Research Papers; 1972.

[23] Vasta M, Pandolfi A, Gizzi A. A fiber distributed model of biological tissues. Proc IUTAM 2013;6:79–86.

[24] Wang Y, Son S, Swartz SM, Goulbourne NC. A mixed von Mises distribution for modelling biological tissues with two distributed fiber properties. Int J Solids Struct 2012;49:2914–2923.